J|A|C|S COMMUNICATIONS

Published on Web 02/05/2010

Synthesis of Pd−Au Bimetallic Nanocrystals via Controlled Overgrowth

Byungkwon Lim,[†] Hirokazu Kobayashi,[†] Taekyung Yu,[†] Jinguo Wang,[‡] Moon J. Kim,[‡] Zhi-Yuan Li,[§] Matthew Rycenga,[†] and Younan Xia*,[†]

Department of Biomedical Engineering, Washington University, St. Louis, Missouri 63130, Department of Materials Science, University of Texas at Dallas, Richardson, Texas 75083, and Institute of Physics, Chinese Academy of Sciences, Beijing 100080, P. R. China

Received November 24, 2009; E-mail: xia@biomed.wustl.edu

Heterogeneous seeded growth represents an effective means of coupling the optical or catalytic properties of one metal with those of another metal, thereby forming multifunctional nanocrystals. Recently, various bimetallic nanostructures consisting of noble metals such as Au, Ag, Pd, and Pt have been explored by this approach, including polyhedral nanocrystals with core−shell structures,[1] anisotropic nanorods with a second metal deposited at their tips,[2] and nanodendrites consisting of branched arms made of one metal supported on a core of another metal.[3] Despite these demonstrations, however, major challenges remain in controlling the mode of overgrowth for a deposited metal, which is a prerequisite for the rational design and synthesis of bimetallic nanocrystals with desired morphology and thus properties. Here we report a facile route to the synthesis of Pd−Au bimetallic nanocrystals with controlled morphology via an aqueous method that involves Pd nanocubes as the seeds. In this work, we demonstrate that two different types of bimetallic nanostructures, namely, core−shell nanocrystals and dimers, can be selectively produced via controlled overgrowth of Au on the well-defined surface of the cubic Pd seeds by a judicious choice of the reducing agent for the synthesis. Using this approach, we were able to not only control the morphology of the Pd−Au bimetallic nanostructures but also tune their localized surface plasmon resonance (LSPR) peaks in the visible region.

Pd nanocubes with an average edge length of 10 nm were synthesized in an aqueous solution by reducing Na_2PdCl_4 with L-ascorbic acid in the presence of bromide ions as the capping agents to promote the formation of {100} facets, as reported previously[4] (Figure S1 in the Supporting Information). We first synthesized Pd−Au bimetallic nanocrystals by reducing $HAuCl_4$ with L-ascorbic acid in the presence of cubic Pd seeds in an aqueous solution. Figure 1A−C shows typical transmission electron microscopy (TEM) images of the products prepared using different concentrations of $HAuCl_4$. In all cases, conformal overgrowth of Au on the Pd nanocubes generated Pd−Au nanocrystals with a core−shell structure. The high-angle annular dark-field scanning TEM (HAADF-STEM) image in Figure 1D shows a clear contrast between the Pd core and the Au shell, confirming the core−shell structure (also see Figure S2). The Pd cores retained their original cubic shape, indicating that they were intact during the deposition of the Au shells. Figure 2A shows a high-resolution TEM (HRTEM) image of a Pd−Au core−shell nanocrystal prepared at a relatively low concentration of $HAuCl_4$ (see Figure 1A). The Au overlayer completely covered the main faces of the Pd nanocube, and its thickness was extremely thin, on the scale of 1−2 nm. The HRTEM image also revealed the continuous lattice fringes from the Pd core to the Au shell, indicating an epitaxial relationship between these two metals. The {100} fringes in the Pd and Au regions showed periods of 1.94 and 2.02 Å, as expected for face-centered cubic (fcc) Pd and Au, respectively. Because of the close matching between the {100} lattice spacings of Pd and Au (∼4% mismatch), the Au atoms could nucleate and grow epitaxially from the {100} surface of a Pd nanocube. As shown in Figure 1B,C, the Au shells increased in thickness to 3−5 nm as the $HAuCl_4$ concentration was increased, demonstrating the feasibility of our approach for the synthesis of Pd−Au core−shell nanocrystals with a controllable shell thickness.

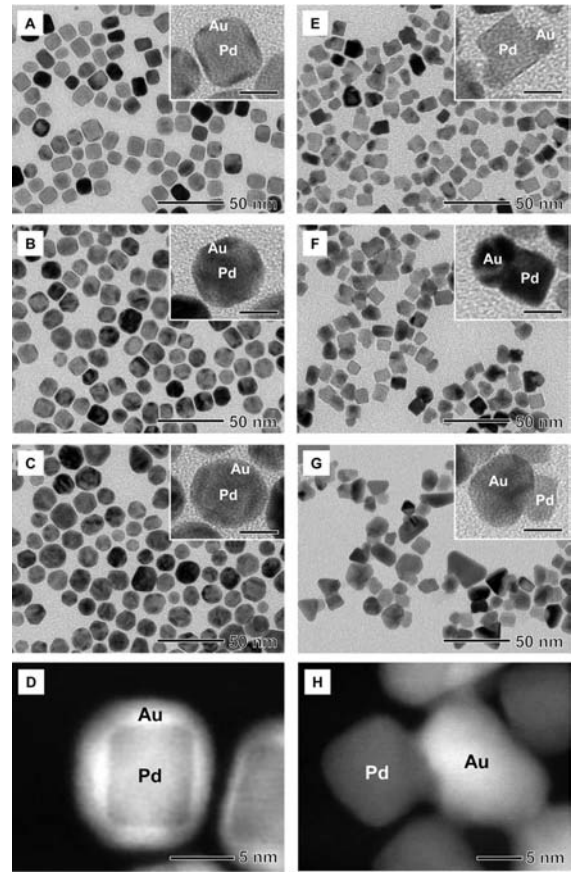

Figure 1. (A−C) TEM images of Pd−Au core−shell nanocrystals synthesized by reducing $HAuCl_4$ with L-ascorbic acid at different concentrations of $HAuCl_4$: (A) 0.53, (B) 0.80, and (C) 1.33 mM. (D) HAADF-STEM image of a Pd−Au core−shell nanocrystal. (E−G) TEM images of Pd−Au nanocrystals synthesized by reducing $HAuCl_4$ with citric acid at different concentrations of $HAuCl_4$: (E) 0.16, (F) 0.27, and (G) 0.80 mM. (H) HAADF-STEM image of a Pd−Au dimer consisting of a Pd nanocube and a Au nanoparticle. All of the scale bars in the insets of the TEM images correspond to 10 nm.

[†] Washington University.
[‡] University of Texas at Dallas.
[§] Chinese Academy of Sciences.

10.1021/ja909787h

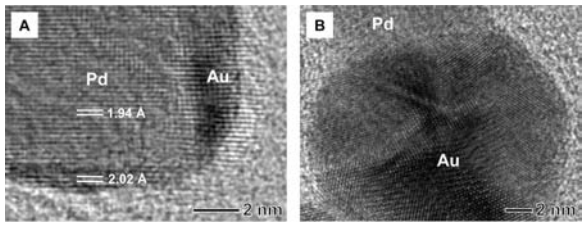

Figure 2. (A) HRTEM image of one of the Pd−Au core−shell nanocrystals shown in Figure 1A. (B) HRTEM image of a Pd−Au dimer, showing the partial decahedral structure of a Au particle attached to a Pd nanocube.

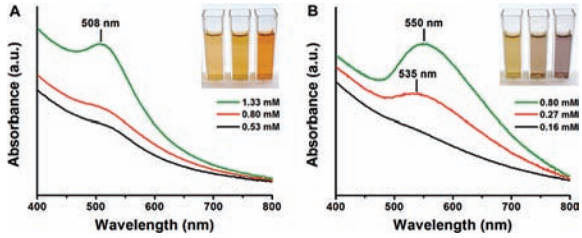

Figure 3. Absorbance spectra and photographs (insets) of aqueous suspensions of Pd−Au nanocrystals synthesized with (A) L-ascorbic acid and (B) citric acid as the reducing agent at different concentrations of $HAuCl_4$ as indicated on each panel. In each photograph, the concentration of $HAuCl_4$ increases from left to right.

Interestingly, the reduction of $HAuCl_4$ by citric acid resulted in localized overgrowth of Au on the Pd nanocubes (Figure 1E−G). At a relatively low concentration of $HAuCl_4$, we observed the formation of single or multiple Au bump(s) with sizes of 5−7 nm on each Pd nanocube, as shown in Figure 1E. HRTEM analysis revealed that these bumps were grown epitaxially on the Pd nanocubes (Figure S3). At a relatively high concentration of $HAuCl_4$, however, overgrowth of Au proceeded only at a single site on each Pd nanocube (see Figure 1G−H), producing bimetallic dimers. This kind of transition from multiple-site to single-site growth has been observed in the deposition of Au tips on Pd or CdSe nanorods, and Ostwald ripening driven by the size difference in Au deposits has been suggested as a mechanism to account for this phenomenon.[2a,5] In the Pd−Au dimers, the Au particles were dominated by either a partial decahedral or platelike morphology (also see Figure S4). The HRTEM image in Figure 2B shows a fivefold-twinned, partial decahedral structure of the Au particle attached to a Pd nanocube. These observations suggest that citric acid may play a significant role in stabilizing the {111} facets of the deposited Au particles, promoting their growth into a decahedral or platelike structure whose surfaces are enclosed by {111} facets.

Figure 3 shows the absorption spectra recorded from aqueous suspensions of the as-synthesized Pd−Au nanocrystals. For comparison, in Figure S5 we have shown the absorption spectrum of the Pd nanocubes, which gave no LSPR peak in the visible and near-IR regions. For the Pd−Au core−shell nanocrystals, the LSPR peak associated with Au shells was observed at 508−515 nm. On the other hand, for the Pd−Au samples prepared with citric acid, the LSPR peak associated with the deposited Au (i.e., small bumps or large particles) appeared at longer wavelengths (>530 nm). The peak was red-shifted to 550 nm as the deposited Au evolved from small bumps into large particles, reflecting the size sensitivity of the LSPR peak of Au nanostructures. For the Pd−Au core−shell nanocrystals, the occurrence of the LSPR peak at a shorter wavelength is intriguing. A comparison of theoretical spectra calculated using Mie theory revealed that the LSPR peak of a Pd−Au core−shell nanocrystal occurs at a shorter wavelength than those of hollow and solid Au nanostructures with the same outer diameter (Figure S6), clearly indicating that the LSPR for Au is blue-shifted as a result of the incorporation of a Pd core. This phenomenon can be attributed to the increase in surface electron density in the Au shell, which is driven by electron donation from Pd to Au because of the higher electron chemical potential of Pd relative to Au.[6] The photographs clearly show the variation in color depending on the morphology of the Pd−Au nanocrystals (Figure 3 insets). These results demonstrate that the optical properties of Pd−Au bimetallic nanostructures can be tuned in a quite different manner by controlling the mode of Au overgrowth.

In previous work on seeded growth of bimetallic nanocrystals, physical parameters such as lattice match, correlation of surface and interfacial energies, and difference in electronegativity between the two metals have been considered as major factors that govern the mode of heterogeneous nucleation and growth.[1−3] Our results suggest that chemical species such as a reducing or capping agent involved in the synthesis may also play an important role in the overgrowth process. The Pd−Au bimetallic nanocrystals reported herein, which combine the properties of both Pd and Au, could serve as promising candidates for both fundamental study of the catalytic properties[7] and applications including in situ monitoring of catalytic reactions via surface-enhanced Raman scattering.[1d,8] We expect that this synthetic strategy could also be extended to other bimetallic systems.

Acknowledgment. This work was supported in part by the NSF (DMR-0804088) and startup funds from Washington University. Part of the work was performed at the Nano Research Facility (NRF), a member of the National Nanotechnology Infrastructure Network (NNIN), which is supported by the National Science Foundation under Award ECS-0335765. J.W. was supported by a grant from CNMT (08K1501-01210) under the 21st Frontier R&D Program of the MEST, Korea.

Supporting Information Available: Experimental procedures, TEM and HRTEM images, absorption spectrum of Pd nanocubes, and theoretical spectra from Mie calculations. This material is available free of charge via the Internet at http://pubs.acs.org.

References

(1) (a) Habas, S. E.; Lee, H.; Radmilovic, V.; Somorjai, G. A.; Yang, P. *Nat. Mater.* **2007**, *6*, 692. (b) Fan, F.-R.; Liu, D.-Y.; Wu, Y.-F.; Duan, S.; Xie, Z.-X.; Jiang, Z.-Y.; Tian, Z.-Q. *J. Am. Chem. Soc.* **2008**, *130*, 6949. (c) Lim, B.; Wang, J.; Camargo, P. H. C.; Jiang, M.; Kim, M. J.; Xia, Y. *Nano Lett.* **2008**, *8*, 2535. (d) Lee, Y. W.; Kim, M.; Kim, Z. H.; Han, S. W. *J. Am. Chem. Soc.* **2009**, *131*, 17036.

(2) (a) Camargo, P. H. C.; Xiong, Y.; Ji, L.; Zuo, J. M.; Xia, Y. *J. Am. Chem. Soc.* **2007**, *129*, 15452. (b) Seo, D.; Yoo, C. I.; Jung, J.; Song, H. *J. Am. Chem. Soc.* **2008**, *130*, 2940.

(3) (a) Zhou, S.; McIlwrath, K.; Jackson, G.; Eichhorn, B. *J. Am. Chem. Soc.* **2006**, *128*, 1780. (b) Lim, B.; Jiang, M.; Camargo, P. H. C.; Cho, E. C.; Tao, J.; Lu, X.; Zhu, Y.; Xia, Y. *Science* **2009**, *324*, 1302. (c) Peng, Z.; Yang, H. *J. Am. Chem. Soc.* **2009**, *131*, 7542.

(4) Lim, B.; Jiang, M.; Tao, J.; Camargo, P. H. C.; Zhu, Y.; Xia, Y. *Adv. Funct. Mater.* **2009**, *19*, 189.

(5) Mokari, T.; Sztrum, C. G.; Salant, A.; Rabani, E.; Banin, U. *Nat. Mater.* **2005**, *4*, 855.

(6) (a) Mei, D.; Hansen, E. W.; Neurock, M. *J. Phys. Chem. B* **2003**, *107*, 798. (b) Sárkány, A.; Geszti, O.; Sáfrán, G. *Appl. Catal., A* **2008**, *350*, 157. (c) Jana, D.; Dandapat, A.; De, G. *J. Phys. Chem. C* **2009**, *113*, 9101.

(7) (a) Chen, M.; Kumar, D.; Yi, C.-W.; Goodman, D. W. *Science* **2005**, *310*, 291. (b) Enache, D. A.; Edwards, J. K.; Landon, P.; Solsona-Espriu, B.; Carley, A. F.; Herzing, A. A.; Watanabe, M.; Kiely, C. J.; Knight, D. W.; Hutchings, G. J. *Science* **2006**, *311*, 362.

(8) Pergolese, B.; Muniz-Miranda, M.; Bigotto, A. *Vib. Spectrosc.* **2008**, *48*, 107.

JA909787H